

LONG-RANGE AND HEAD-ON BEAM-BEAM INTERACTIONS : WHAT ARE THE LIMITS?

X. Buffat, G. Arduini, E. Bravin, G. Iadarola, E. Métral, Y. Papaphilippou, D. Pellegrini, S. Redaelli, B. Salvachua, M. Solfaroli, G. Trad, D. Valuch, J. Wenninger, CERN, Geneva, Switzerland
J. Barranco, T. Pieloni, C. Tambasco, EPFL, Lausanne, Switzerland
M. Crouch, University of Manchester, England

Abstract

The present understanding of the performance limitations due to beam-beam interactions in the LHC is detailed based on data obtained during the physics run as well as dedicated experiments in 2016.

INTRODUCTION

The effect of beam-beam interactions manifests itself as a deterioration of the beam quality through various mechanisms. The understanding of these mechanisms is crucial in order to operate the machine in optimal conditions. The best performance is obtained in conditions that maximise the physics reach of the different experiments with different needs. In particular, the need for dynamic control of the luminosity, or levelling, in the different experiments, together with the operational constraints given by the control system and the machine protection needs to be taken into account in the understanding of the beam-beam driven limitations on the performance.

In the following section the effects of long-range beam-beam interactions observed in 2016, as well as the operational strategy for the setting up of the crossing angle and β^* w.r.t long-range limitations is exposed. Dedicated tests to probe the limitations linked to strong head-on beam-beam effects are detailed in the third section. The effect of luminosity levelling with a transverse offset in both the low and high luminosity IPs are discussed in the fourth and fifth sections respectively. The emphasis is put on experimental data, detailed simulations and extrapolations to future scenarios are discussed in [1].

LONG RANGE INTERACTIONS

Crossing angle scans

In order to evaluate experimentally the minimum crossing angle at which the LHC can be operated in given conditions, the crossing angle in the two main IPs are reduced simultaneously in steps. The steady state losses measured at each of these steps are reported in Fig. 1, averaged over bunches experiencing different number of long-range interactions. The detrimental effect of the non-linearities of long-range interactions is most significant on bunches experiencing a larger number of interactions [2]. For beam 1, we observe that the decay rates are identical for all bunches for half crossing angle larger than $130 \mu\text{rad}$, the losses are therefore not driven by long-range beam-beam effects. At smaller crossing angles, nominal bunches (pink) lose more than the

other bunches. This angle correspond to the onset of long-range driven losses, which risk to compromise the integrated luminosity by reducing significantly the beam lifetime in collision as experienced for example during the 2012 proton Run [3, 4]. The strength of the long-range interactions is well characterised by the bunch intensity and the normalised separation between the beams at the location of the interaction given for the interactions in the drift space around the IP given by :

$$S_{\text{drift}} \approx 2 \sqrt{\frac{\beta^* \gamma_r}{\epsilon_n}} \theta, \quad (1)$$

with θ the half crossing angle. The onset of long-range driven losses was therefore measured at a crossing angle corresponding to a normalised separation of 8.6σ for a bunch intensity of $1.2 \cdot 10^{11}$. In beam 2, long-range driven losses were visible below $105 \mu\text{rad}$, corresponding to a normalised separation of 7σ . The asymmetry between the beams is not fully understood, nevertheless a significant tune shift was observed in beam 1 when reducing the crossing angle. By comparing the spectrogram of the bunch colliding head-on only (Fig. 2a) and those colliding long-range in IPs 1 and 5 (Fig. 2b), it is clear that the tune shift is not due to a drift of the machine tune, but is driven by long-range interactions. The shift increases the vertical tune shift towards the third, as well as few other detrimental long-range driven higher order resonances, which could explain the losses observed in the vertical plane of beam 1 shown in Fig. 2c [5].

The measured variations show an increase of the vertical tune simultaneous to a decrease of the horizontal tune. Such effect is expected for a tune shift driven by long-range interactions, but should however be cancelled by the passive compensation between IPs 1 and 5, due to the alternating crossing angle in the horizontal and vertical plane [6]. Consequently the observations suggest that the passive compensation is broken, either due to a difference between β^* in the two IPs, or a difference in crossing angle.

The presence of uncompensated long-range driven tune shifts were confirmed in another experiment [7], where a single low intensity bunch in beam 1 collided against a full 48 bunch train in IPs 1 and 5. While the crossing angle was reduced, beam transfer functions were measured on the low intensity beam. The tune shift as well as an estimation of the transverse tune spread are reported in Fig. 3, based on a fit of the measurements [8].

A relative difference in the order of 30% [9] shared between the crossing angle and the β^* would explain the measured tune shifts. However neither the β^* [10] nor the measured

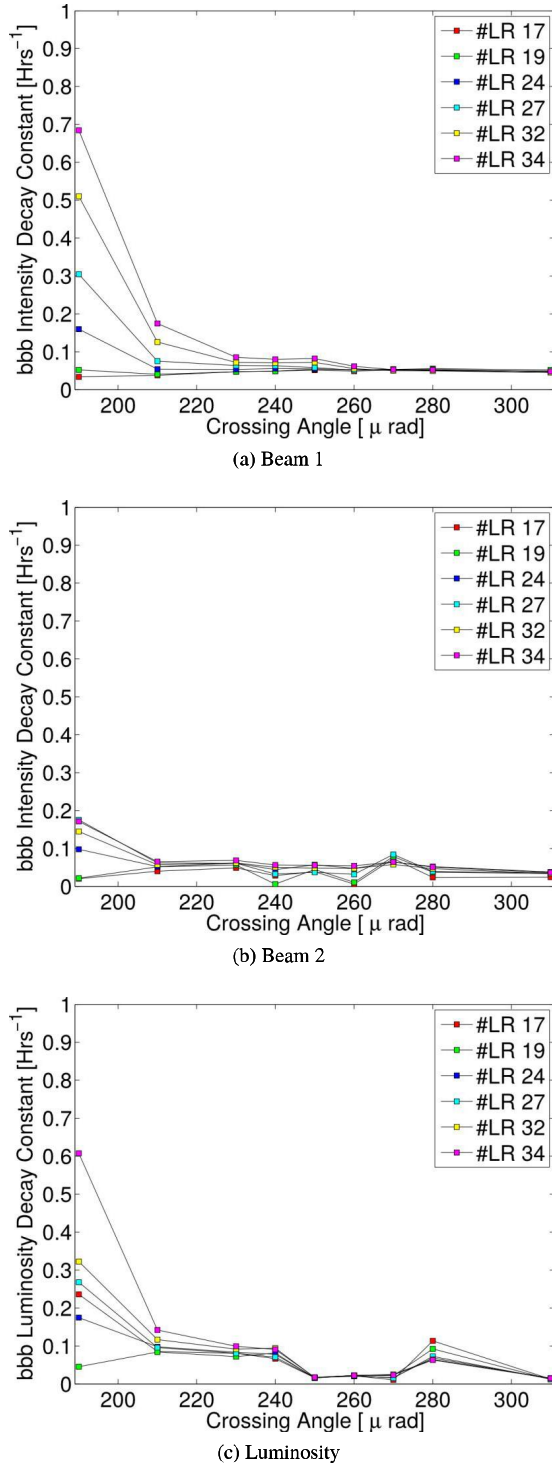


Figure 1: Intensity and luminosity decay rates averaged over bunches with identical number of long-range beam-beam interactions in IPs 1 and 5, while reducing simultaneously the full crossing angles.

nominal crossing angle [11] are compatible with measurements. The presence of significant coupling at the location of long-range interactions at one or the other IP could also generate such an effect and is not incompatible with local coupling measurement [12]. Since the passive compensation is an important mechanism to obtain a good dynamic aperture, it is likely that by understanding the mechanism and restoring the compensation, the impact of long-range interactions could be reduced. Dedicated orbit and optics measurement, including local coupling, would be needed.

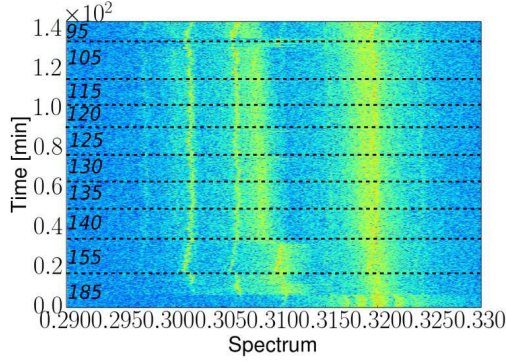
Observation during operation

The onset of losses observed in dedicated experiments in 2016 is consistent with the 8.4σ obtained in 2015 in similar conditions [4]. The crossing angle for the 2016 Run ($185 \mu\text{rad}$) was chosen based on those experiments, assuming an emittance in collision of $3.5 \mu\text{m}$ and including a margin of 2σ to allow for operational margins on the machine parameters and to account for uncertainties on the beam quality in collision, mainly due to the unknowns on the electron cloud effects at injection. After the implementation of the BCMS scheme, the same crossing angle corresponds to more than 12σ thanks to the reduction of the emittance 3.5 to below $2.5 \mu\text{m}$ [13]. The bunch intensity is also reduced at about 10^{11} protons per bunch. In the period between the implementation of the BCMS scheme and the reduction of the crossing angle, the LHC was operated in relaxed conditions, far from long-range driven limitations. This is consistent with the low level of losses observed in that period [14].

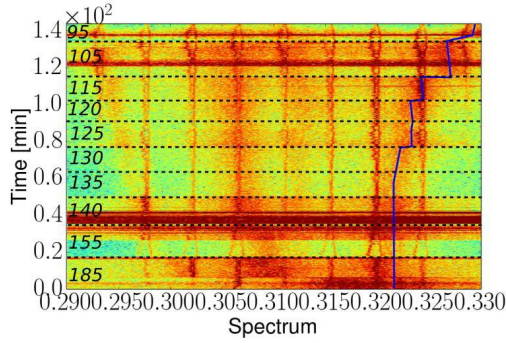
Taking advantage of the reduced emittance and reducing the margins to 1σ with respect to the measured onset of long-range driven losses profiting from the stability of the beam parameters in collision, the half crossing angle could be reduced from $185 \mu\text{rad}$ to $140 \mu\text{rad}$, corresponding to a normalised separation of 9.2σ , with an emittance of $2.5 \mu\text{m}$ [15].

The reduction of the crossing angle led to an increase of the losses in the first fills of operation for physics after the technical stop with a pattern indicating the presence of long-range effects. These losses could however be mitigated by first correcting the long-range induced tune shift that was measured in dedicated experiment, resulting in an improvement to a level of losses similar to prior the crossing angle change, as illustrated by the maximum power loss during ADJUST shown in Fig. 4 [5]. The ADJUST beam process included the reduction of the crossing angle, the implementation of the TOTEM bump as well as the collapse of the separation bump. Even prior to the tune adjustment, the level of losses remained well below the limitation of the collimation system [16].

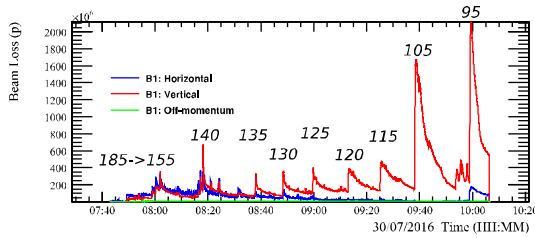
Despite the correction of the uncompensated long-range driven tune shift, the losses in the first hour of stable beam were still significantly higher than prior to the change of crossing angle reducing the performance by few percent [14]. A second step of optimisation of the tunes allowed for a re-



(a) Bunches colliding head-on



(b) Bunches colliding head-on and long-range



(c) Losses

Figure 2: BBQ spectrogram in the vertical plane of beam 1 of different bunches (upper plots) when reducing the crossing angle in IPs 1 and 5. The evolution of the vertical tune peak is highlighted with a blue line, for bunches colliding long-range in IPs 1 and 5 (middle plot), whereas the tune of bunches colliding head-on (top plot) remains steady at 0.32. The losses decomposed by plane during the reduction of the crossing angle are shown in the bottom plot, with the corresponding half crossing angle at the time of the loss spikes.

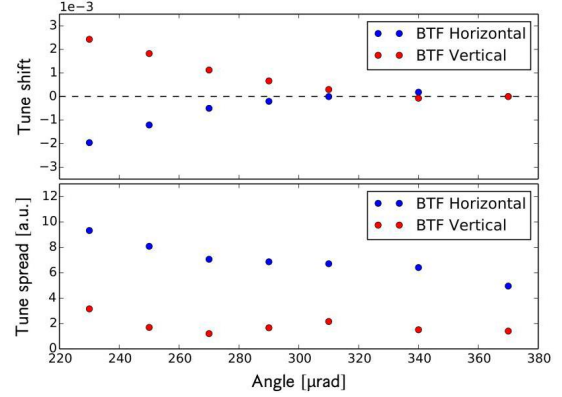


Figure 3: Tune shift and spread measured in beam 1, with a single low intensity bunch colliding long-range against a 48 bunch train in IPs 1 and 5. The parallel separation was kept on to avoid head-on collisions and the crossing angle reduced in steps simultaneously in the two IPs.

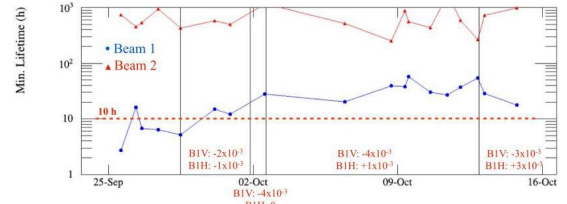


Figure 4: Minimum lifetime drop during the ADJUST process during consecutive fills with different tunes.

duction of the losses in this phase, consistently with dynamic aperture simulations suggesting that the nominal working point is not optimal in such configurations. In absence of coupling, working points closer to the diagonal are expected to perform better, as shown by Fig. 5.

HEAD-ON INTERACTION

Operation with large beam-beam parameters

Previous studies at injection highlighted prohibitive degradation of the luminosity lifetime when colliding with large beam-beam parameters, as reported in Fig. 6. Such a degradation was no longer observed at top energy in dedicated experiments in 2016, reaching a total beam-beam tune shift of -0.02 with collisions in IPs 1 and 5. The beam lifetime was dominated by luminosity burn-off, while the transverse emittances suffered from a growth mechanism resulting in a few percent per hour additional to the effect of intrabeam scattering [20]. These experiments were performed with high intensity bunches, requiring special settings of the transverse damper (ADT). As a result, the noise that the latter introduces was increased. This effect could explain the growth mechanism and will be further discussed in next section.

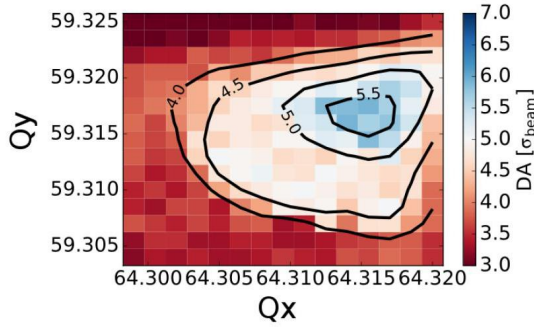


Figure 5: Minimum dynamic aperture simulated with SIX-TRACK over 10^6 turns for the 2016 configuration with reduced crossing angle, an intensity of $1.15 \cdot 10^{11}$ protons per bunch, transverse emittances of $2 \mu\text{m}$, focusing octupoles powered with 500 A and the negative (according to LSA convention) polarity of LHCb.

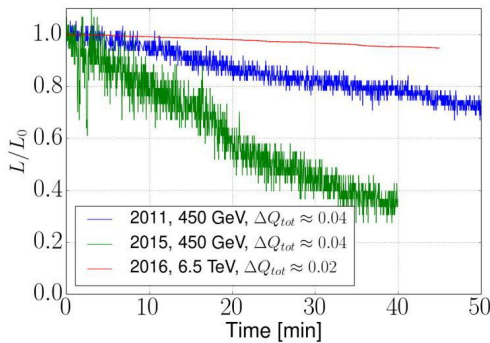


Figure 6: Luminosity evolution during different tests with large beam-beam parameter [17–20].

A strong degradation of the beam quality was observed during the high- β run when colliding beams with large beam-beam tune shift and keeping the injection tunes. When moving to collision tunes, the preservation was restored as expected, resulting in stable operation with beam-beam parameters as large as -0.025 [21]. Due to the significantly different configurations with respect to proton physics, in particular because of the larger β^* and due to the frequent tail scraping in order to minimise the background, a detailed comparison with the proton physics run is difficult.

The effect of external sources of noise

In the presence of a large tune spread within the beam, external sources of noise result in an emittance growth through decoherence. Currently, the emittance evolution in collision can be understood within few percent per hour considering the effect of synchrotron radiations and intrabeam scattering [14]. The remaining is compatible with the effect of external sources of noise acting on the beams with an amplitude normalised to the beam divergence around $8 \cdot 10^{-5}$. The dipole's power converter ripple and

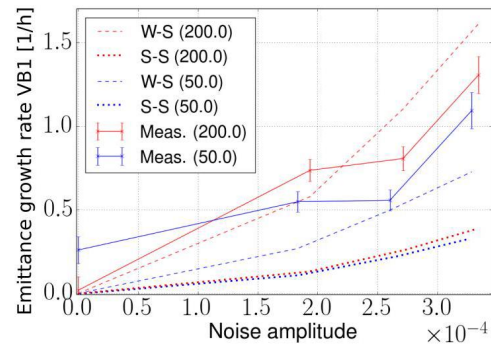


Figure 7: Emittance growth measured on bunches experiencing different ADT gain as a function of the Gaussian white noise amplitude introduced artificially by the ADT kicker (solid line), compared to the expectation of the weak-strong model (dashed) and the strong-strong model (dotted). The corresponding damping time from the ADT is given in the legend.

the ADT are the main potential sources for such a noise. If we were to assume that the noise is dominated by the ADT, a finite resolution of $0.2 \mu\text{m}$ on the measured beam position used in the feedback loop would be sufficient to explain the observations. Further beam tests are needed to evaluate the strength of the different sources, in particular the impact of the ADT can be singled out by varying and optimising its parameters, such as gain and bandwidth.

The strong-strong theory predicts an improvement of the efficiency of the ADT in mitigating the effect of external sources of noise on the emittance. This effect could in principle be used to improve the performance, however it relies on precise machine and beam conditions [22]. A proper understanding of the conditions within which this mechanism can be reliably achieved in the LHC is needed to allow for an optimisation in that respect. By introducing artificially noise using the ADT and varying the beam-beam tune shift as well as the ADT gain, it was shown that the weak-strong theory [23, 24] is in reasonable agreement with the observations. In particular Fig. 7 shows the predictions of the two models along with the measurements, showing that the conditions to profit from the beneficial effects predicted by the strong-strong theory are not met in this configuration. Further tests are needed to try an establish those conditions.

The tests with large beam-beam tune shifts highlighted an important difference in the behaviour of the bunches of different intensities and different ADT gain, already prior to the injection of artificial noise. The data points obtained without artificial noise reported in Fig. 7 illustrate this effect. The bunch experiencing the larger ADT gain is growing more than the others, suggesting that the ADT is the cause for this extra growth. Since the settings of the ADT were not optimal in these tests due to the large

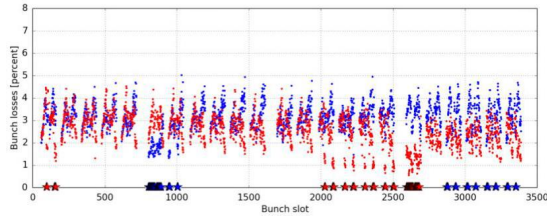


Figure 8: Bunch by bunch loss rate averaged over the first 30 minutes of stable beam during fill 5393, after the reduction of the crossing angle and a swap of the LHCb spectrometer polarity. The contribution of burn off to beam losses was subtracted. The bunches that do not collide head-on in IP8 are designated with a blue or red stars corresponding to beam 1 or beam 2 respectively.

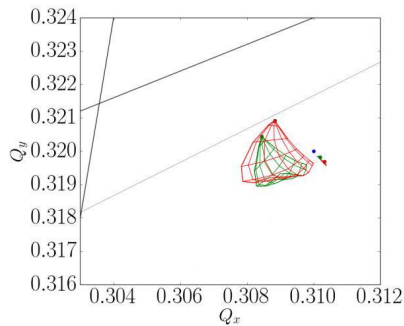


Figure 9: Tune footprint arising from long-range interactions in IP8 (small red and green footprints) and both long-range and head-on interaction (big red and green footprints) for the negative and positive polarity of the LHCb spectrometer respectively (according to LSA convention). The transverse separation is chosen to obtain the same reduction factor, corresponding to the situation at the beginning of a physics fill.

intensities with respect to regular operation, it is not possible to directly extrapolate those results for proton physics operation. However, this highlights the importance of the ADT settings in the observed emittance growth and motivates an optimisation of those parameters in regular physics fills. Keeping in mind that, while the impact on performance is marginal with current machine and beam parameters (the total beam-beam tune shift is around -0.007 in regular operation for proton physics), these effects become significant when pushing the machine and beam parameters (higher sensitivity to quadrupole vibrations with reduced β^* , higher intensities, larger tune spread).

THE IMPACT OF IP 2 AND 8

The long-range effects in IPs 2 and 8 are negligible, thanks to the larger normalised separation with respect to the two main IPs. Indeed, the crossing angle and β^* are

usually set to avoid an uncompensated tune shift and spread higher than 10^{-4} which could result in dynamic aperture reduction [4]. In particular for the 2016 configuration after the reduction of the crossing angle, positive vertical tune shift rapidly result in a reduction of the dynamic aperture, as shown in Fig. 5 [1].

The luminosity is levelled with a transverse offset in both IPs, resulting in total normalised separation between the beams at the IP in the order of 4σ in IP2 and 2σ in IP8 at the beginning of luminosity production. The tune shift and spread due to the interaction at the IP is therefore significantly stronger in IP 8 w.r.t. IP 2. Consistently, no detrimental effects could be linked to the collisions in IP2, however a significant effect of the collisions in IP8 was visible right after the change of crossing angle and of the polarity of the LHCb spectrometer. Bunches without collisions in IP8 experienced less losses in the first hour of stable beam with respect to others in both beams (Fig. 8). The effective crossing angle at the IP is different for the two spectrometer polarities, resulting in different luminosity reduction factor. To achieve the same target luminosity, the initial separation at the IPs is different for the two polarities, resulting in different beam-beam effects. This difference is illustrated with the corresponding tune footprints in Fig. 9. Since, as shown in Fig. 5, the dynamic aperture is particularly sensitive to positive tune shifts in the vertical plane, the increase of the vertical tune shift due to the head-on interaction with an offset at IP8 can explain the increase of the losses when swapping the polarity. Consistently, this effect was no longer visible after the tune optimisation mentioned above [25].

The effect of IP8 did not represent a limitation of the operation in the 2016 Run, since its detrimental effects remained under control and could be mitigated adjusting the tune. Nevertheless, the sensitivity to the tune shift induced by head-on interaction in IPs 2 and 8 could be reduced by levelling the luminosity with equal offsets in the two transverse planes in each of the IPs, resulting in tune shifts along the diagonal and potentially reducing the impact on dynamic aperture and lifetime.

LEVELLING WITH A TRANSVERSE OFFSET IN IPS 1 AND 5

As the LHC outperforms its design in terms of peak luminosity, the need for luminosity levelling to mitigate the high pile up in the two main experiments can not be excluded in a near future. Whereas other levelling schemes such as dynamic modifications of the β^* offer several advantages from the beam dynamics point of view [26], levelling with a transverse offset at the IP appears as the most simple solution from an operational point of view [27]. In particular, it has been already successfully used operationally in the two lower luminosity experiments. Consequently, the procedure was validated operationally for the two high luminosity experiments within regular physics fill. The luminosity was

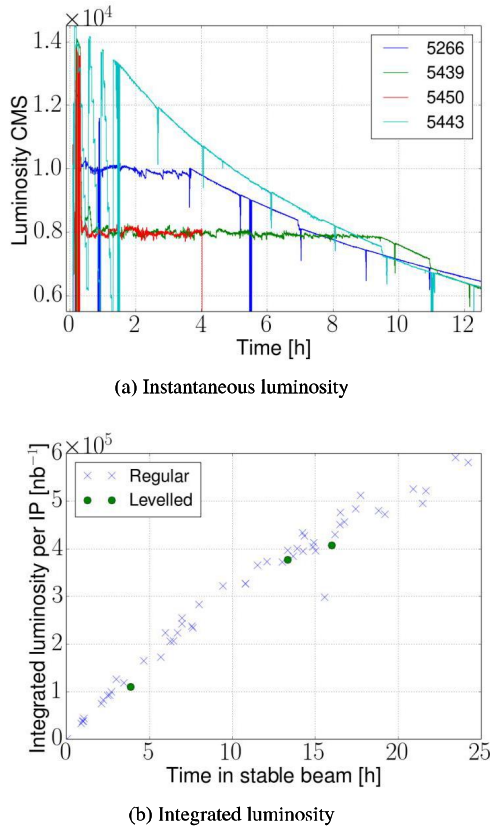


Figure 10: Evolution of the luminosity during the physics fills with a luminosity levelled with a transverse offset at the IP, along with a comparison of the integrated luminosity with physics fill without levelling.

levelled by manually adjusting the orbit at IPs 1 and 5 to obtain a constant luminosity of $10^{34} \text{ cm}^{-2}\text{s}^{-1}$ in the first test and $8 \cdot 10^{33}$ in the second and the fourth tests. The luminosity during those tests is shown in Fig. 10, along with the corresponding integrated luminosity as a function of the time spent in stable beam. The latter allows for a comparison with other physics fills. Assuming a luminosity evolution only driven by luminosity burn-off, one expects a loss of integrated luminosity of 10 % for the last two tests. Within the uncertainty due to the fill to fill variation of the beam parameters, the integrated luminosity obtained during the test is in agreement with the expectation, showing that the levelling scheme did neither cause significant additional mechanisms deteriorating the beam quality, nor mitigated the ones present without levelling. Yet, a more detailed comparison of the beam losses during the fill shows an increase of the losses in the first hour in the first and second tests. These losses were mitigated profiting from the stability margins that were demonstrated in another test (fill 5443 in Fig. 10a). The current in the octupoles could be reduced from 470 A to 220 A and the chromaticity reduced from 15 to 10 units, without experiencing any instabilities while varying the separation at the IPs in the range of interest. The implementation of

these reductions, together with a tune optimisation allowed to recover beam losses similar to regular physics fills in the last test (fill 5450).

CONCLUSION

The operational crossing angle and β^* are usually defined before the start of the physics run, based on the observed reduction of the beam lifetime when reducing the crossing angle in dedicated experiments with similar machine and beam parameters, as well as comparison and extrapolations using dynamic aperture simulations. Significant margins with respect to the fundamental limit are needed due to uncertainties on the beam parameters in collision, to allow for operational flexibility during the recommissioning and in some cases due to the inherent uncertainties in the beam dynamics model when extrapolating experimental data obtained in different conditions. For the first time, the crossing angle was reduced during the proton run in the LHC, not only profiting from the reduced emittance with BCMS beams but also from the relaxing of the margins that were no longer needed allowing to operate closer to the long-range limit. The success of this operation motivates operational efforts towards more flexibility in the control of the crossing angles during the physics run.

When operating closer to the long-range limit, subtle effects become relevant. A good understanding of the interplay between both the low and high luminosity IPs, of the optics at the location of the beam-beam interactions, the effect of the chromaticity and the octupole settings have a significant impact on the beam dynamics. These detrimental effects could be observed in different conditions during the 2016 Run, yet they remained under control in terms of beam quality degradation and beam losses. These observations and their comparison to beam dynamics models, in particular to dynamic aperture simulation, allowed for a deeper understanding of the machine, nevertheless discrepancies observed in the measured tune and tune spread when reducing the crossing angle suggest that the long-range limit is not yet entirely understood.

Currently, the head-on beam-beam interactions do not limit the operation of the LHC, experimental tests were conducted to probe these limitations with single bunches of high brightness. Total beam-beam tune shifts in the order of 0.02 were reached and the beams were showing an excellent lifetime. The transverse emittances were, however, significantly affected. The effect of external sources of noise needs to be further investigated in order to define limitations for future scenarios with pushed machine and beam parameters.

Levelling the luminosity with a transverse offset in the two main experiments was demonstrated with regular physics beam and therefore could be used if needed during the next runs, keeping in mind that beam-beam interactions with an offset lead to an important tune shift that may have an impact

on the beam lifetime. These tune shifts are passively mitigated by alternating the levelling plane of the two high luminosity IPs. In order to profit from this effect, the two experiments are required to level at the same target luminosity. In case this condition is not met the potential of different options in terms of crossing planes should be studied.

REFERENCES

- [1] T. Papaphilippou. “Scenarios for 2017 and 2018.” In: *these proceedings*.
- [2] M. Crouch et al. *Long range beam-beam interaction and the effect on the beam and luminosity lifetimes*. Tech. rep. In preparation. Geneva, Switzerland: CERN, 2017.
- [3] T. Pieloni et al. “Stability of Colliding Beams at 6.5TeV.” In: *Proceedings of the 2012 Evian workshop on LHC beam operation*. Ed. by B. Goddard and S. Dubourg. Evian-les-Bains, France: CERN.
- [4] T. Pieloni et al. “Beam-beam effects long-range and head-on.” In: *Proceedings of the 2015 Evian workshop on LHC beam operation*. Ed. by B. Goddard and S. Dubourg. Evian-les-Bains, France: CERN.
- [5] B. Salvachua et al. *Beam losses during crossing angle change*. Presentation at the LHC Beam Operation Committee, 18. Aug 2016.
- [6] W. Herr. *Features and implications of different LHC crossing schemes*. Tech. rep. LHC Project Report 628. Geneva, Switzerland: CERN, Feb. 2003.
- [7] C. Tambasco et al. *MD 1856 - Landau Damping: Beam Transfer Functions and diffusion mechanisms*. Tech. rep. In preparation. Geneva, Switzerland: CERN, 2017.
- [8] C. Tambasco et al. *BTF measurements in the LHC: some updates on the analysis*. Presentation at the HSC section meeting, Jan. 2017.
- [9] C. Tambasco et al. *BTF what’s new in 2017?* Presentation at the MD Day 2017, 31 Mar. 2017.
- [10] T. Persson et al. “Optics control in 2016.” In: *these proceedings*.
- [11] M. Hostettler and J. Wenninger. *Crossing angle from K-modulation*. Presentation at the Optics Measurement and Correction meeting, 7 Feb. 2017.
- [12] R. Tomas. Private communication, Dec. 2017.
- [13] M. Hostettler et al. “How well do we know our beams?” In: *these proceedings*.
- [14] F. Antoniou et al. “Can we predict luminosity?” In: *these proceedings*.
- [15] T. Pieloni et al. *BBLR studies and possible reduction of the crossing angles in the LHC*. Presentation at the LHC Machine Committee, 31. Aug 2016.
- [16] B. Salvachua and S. Redaelli. “Analysis of beam losses.” In: *these proceedings*.
- [17] R. Alemany et al. *Head-on beam-beam tune shifts with high brightness beams in the LHC*. Tech. rep. CERN-ATS-Note-2011-029 MD. Geneva, Switzerland: CERN, June 2011.
- [18] M. Albert et al. *Head-on beam-beam collisions with high intensities and long range beam-beam studies in the LHC*. Tech. rep. CERN-ATS-Note-2011-058 MD. Geneva, Switzerland: CERN, July 2011.
- [19] J. Barranco et al. *MD 402: Head-on limits. Separation levelling*. Tech. rep. CERN-ACC-NOTE-2016-0023. Geneva, Switzerland: CERN, Jan. 2016.
- [20] X. Buffat et al. *Limitations due to strong head-on beam-beam interactions*. Tech. rep. In preparation. Geneva, Switzerland: CERN, 2017.
- [21] H. Burkhardt. *The LHC perspective, including a first assessment of the implications of these requests, also based on the experience accumulated so far*. Special Joint LPC/LPCC meeting on the LHC forward physics programme (Run-2 and beyond), 31 Oct. 2016.
- [22] Y. Alexahin. “A study of the coherent beam-beam effect in the framework of Vlasov perturbation theory.” In: *Nucl. Instrum. Methods Phys. Res. A* 480.2 (2002), pp. 253–288.
- [23] V.A. Lebedev. “Emittance growth due to noise and its suppression with the feedback system in large hadron colliders.” In: *AIP Conf. Proc* 326.396 (1995), pp. 396–423.
- [24] X. Buffat et al. *Probing the behaviour of high brightness bunches in collision at 6.5 TeV and the interplay with an external source of noise*. Tech. rep. In preparation. Geneva, Switzerland: CERN, 2017.
- [25] D. Pellegrini et al. *Report on Beam 1 Lifetime Recovery*. Presentation at the LHC Machine Committee, 19. Oct 2016.
- [26] X. Buffat et al. “Beam-Beam Effects in Different Luminosity Levelling Scenarios for the LHC.” In: *Proceedings of 5th International Particle Accelerator Conference*. Ed. by C. Petit-Jean-Genaz et al. Dresden, Germany: JACoW, 15–20 June 2014 2014, pp. 1061–1063.
- [27] K. Fuchsberger. *Levelling option (if needed)*. Presentation at the LHC Performance Workshop 2017, 24 Jan. 2017.

